## Minitomography Scanner for Agriculture Based on Dual-energy Compton Scattering

PAULO E. CRUVINEL <sup>1</sup>
FATAI A. BALOGUN <sup>2</sup>

<sup>1</sup>Embrapa Agricultural Instrumentation, P.O.Box 741, 13560-970 São Carlos-SP, Brazil cruvinel@cnpdia.embrapa.br

<sup>2</sup>Physics Department, Obafemi Awolowo University, Ile-Ife, Nigeria.

**Abstract.** This paper presents a new approach in tomographic instrumentation for agriculture based on dual-energy Compton scattering. Result shows a linear relationship independent of soil aggregate sizes with regression coefficient of better than 0.95 for bulk density and 0.70 for water content. A minimum detectable density of 0.13g/cm<sup>3</sup> and 0.10 cm<sup>3</sup>/cm<sup>3</sup> were observed with better than 2% and 5% precision respectively. Compton scatter images of soil samples illustrating the efficacy of this imaging technique are presented.

#### 1 Introduction

Nondestructive-testing practitioners challenged complex products can choose sophisticated methods and systems, such as computerized tomography, emission tomography or one of several magnetic resonance imaging systems developed for other applications. Computerized tomography (CT) a technique pioneered by Cormack [1] and Hounsfield [2] permits imaging of objects in axial cross sections. These images can then be stored as a stack of two-dimensional (2D) matrices of numbers [3]. Despite the proven success of these techniques in diverse fields, studies of applications of scattered photons have continued to gain momentum within the past decade. Both coherently and incoherently scattered photons and a technique employing the energy profile of Compton scatter peaks have been used variously and in combination to characterize body tissues such as bones, soft tissues, lung and fats [4-7]. Compton scattering measurements have found applications such as quality control in manufacturing machine tools, and automotive parts, as well as for monitoring high temperature environment of molten metals [8-11]. In all these cases, the compactness of the required instrumentation allows placement of both source and detector on the same side of the object whose density is to be measured. Use of back-scattering angles has been shown to improve the sensitivity [7] and enhance the reproducibility of measurement [8].

Apart from single-point densitometry, density mapping of a plane of interest (imaging) has been performed on various objects [12-14]. The advantages often cited include, for various reasons, partial body accessibility, imaging, and reduced need for reconstruction. computational image However. applicability of this technique had been limited due to a number of factors. These include systematic uncertainties as to attenuation of both incident and scattered beam of photons in the object, contribution of multiply scattered photons to the useful signal, and scattering volume from which the useful signal is derived. Recently, Balogun and collaborators have studied the variation of scattering volume with scattering angle using a numerical-analysisbased computer algorithm [11][15].

In a recent study by Shakestaff et al. [4], the thickness dependence of scattered photon fluency was demonstrated for an epoxy-resin sample examined at 150° scattering angle using the 60keV photon energy of <sup>241</sup>Am. A value of 5cm was obtained for the saturation thickness.

X-ray computerized tomography (CT), one of

several types of direct transmission tomographic systems applied by Embrapa Agricultural Instrumentation Center since 1984, is now recognized as a versatile technique by both soil science and various industrial sectors. In the present study, designed to overcome problems incurred by direct transmission tomography methods, we report results of a dedicated dual-energy Compton scattering minitomography scanners, developed for agricultural applications.

## 2 Computerized Tomography in Soil Science

Computerized tomography, as a new investigatory method in soil science physics, was introduced by Petrovic et al. [16] in 1982, Hainsworth and Aylmores in 1983 [17], and Crestana et al. in 1984 [18]. Petrovic demonstrated the possibility of using X-ray transmission computed tomography to measure soil bulk density. Crestana showed that CT can also be applied not only for measuring water content of soil but also to follow dynamically in three dimensions motion water in soil. Also, using a third-generation CT scanner, techniques such as differential tomography and real time and space distribution scanning modes can be applied. A linear dependence was demonstrated for the Hounsfield units (HU) used in CT and water content.

Application of CT methodology in soil science has proven nighly advantageous when compared to other classical methods such as gravimetry or γ-ray direct transmission [19]. Using CT makes possible either measuring local heterogeneity within the soil at pixel resolution or soil bulk density and water content pixel by pixel, or even to non-invasively obtain two- and three-dimensional images of soil samples independent of sample's geometry and shape. Two- and three-dimensional measurement of soil physical parameters such as bulk density and water content is an important task in modeling and analyzing soil science problems. In agriculture, a need exists for nondestructive experimental

techniques having millimeter or sub-millimeter resolution capable of investigating the intricacies of the many processes occurring in soils. Some examples of coupled and time-dependent soil processes are compaction, root penetrations, crusting, seedling cracking and swelling, wetting and drying or thawing and freezing cycles, miscible and immiscible displacement of nutrients in the presence of roots, and preferential flow of pollutants in fractured porous media. Continuing CT's evolution into a powerful tool for studying such soil phenomena, in 1987 Cruvinel et al. [20,21] developed for multidisciplinary use a direct transmission X and γ-ray computerized minitomograph scanner able to use several different beam energies from radioactive sources as well as X-rays from fluorescent targets.

However, in all these techniques demand unlimited access to the object under examination from opposite newpoints. In cases where this requirement could not be met, as it is in-situ measurement of soil physical parameters, other methods could prove useful. One of these is Compton Backscatter tomography, allowing bath source and detector to be fixed on the same side of the object.

# 3 Principles of the Dual-energy Compton Scattering Tomographic Method

In interacting with matter, including soil, an incident gamma or X-ray undergoes one of mutually probable interactions, chief of which are coherent scattering, incoherent scattering, photoelectric effect, and pair production. Which of these interactions the predominating is interaction a function of photon incident energy. In photoelectric interaction, the energy of the incoming photon is completely absorbed by an orbital electron, while a partial energy loss is suffered by the photon as it undergoes an incoherent scattering with a virtually free electron. In the latter case, the photon's energy is shared by the target electron and the scattered photon. In the case

of pair production, an incident photon, in the presence of a nuclear field, is converted to an electron and a positron pair. Interaction, via the coherent scattering route entails no loss of energy by the incident photon.

Apart from the energy dependence, influence of the modes of interaction is modulated according to the atomic number Z of the target elements.

If the partial interaction probabilities of the various modes of interaction modes are plotted against photon energies, the range of influence of each mode is clearly apparent. This shows that below 30keV photon energy, photoelectric effect is dominant with coherent scattering showing some contribution. Above this level and up to 60keV is a mixture of photoelectric, coherent and incoherent scattering. In the range 60keV to a few

MeV range, however, incoherent scattering takes over as the dominant mode of gamma interaction in soil. Pair production begins at 1.22MeV threshold becoming relevant only at several MeV of photon energy.

It is thus clear that within the limits of gamma ray energies, i.e., 60keV and 1.33MeV, from commercially available radioisotopes, the predominant interaction by far mode of gamma rays in soil is the incoherent or Compton scattering. When in Compton scattering predominates, the Klein-Nishina differential cross section is valid for a free electron; a unique function of angle, it is given by:

$$\frac{d_e \sigma^{KN}(E)}{d\Omega} = \frac{r_0^2}{2} \left[ \frac{1 + \cos^2 \theta}{(1 + \alpha(1 - \cos \theta))^2} \left[ 1 + \frac{\alpha^2 (1 - \cos \theta)^2}{(1 + \cos^2 \theta)(1 + \alpha(1 - \cos \theta))} \right] \right]$$

where  $r_0$  is the classical electron radius numerically equal to 2.818 x  $10^{\cdot 15}$  m, and  $\alpha$  is the rate between the energy E of the incident photon and the rest mass energy of the electron, which is equal to 511keV.

The validity of this equation rests on photon energy being much greater than the target's binding

energy, with the number of scattered photons for each expected to be proportional to bulk density or water content. More concretely the beams of incident and scattered photons suffer attenuation in travelling from the source through the sample to the scattering volume and thence to the detector. To account for these, we can express the number of singly scattered photons noted by the detector during a counting time of t seconds as:

$$S(E) = I_0(E)t\varepsilon \exp\left(-\int_{x_1} \mu_1(x, E)dx\right) \frac{d_e \sigma^{KN}(E)}{d\Omega} \rho \frac{N_A Z}{A} \exp\left(-\int_{x_2} \mu_2(x, E)dx\right) dV d\Omega$$

where  $I_0(E)$  is the incident photon flux with energy E;  $\rho$  is the bulk density; Z is the atomic number; N is the Avogrado's number and  $N_A$  is the mass number of the material under investigation. Here,  $\epsilon$  is the detector's photopeak counting efficiency at the scattered photon energy;  $x_1$  and  $x_2$  represent the length of the paths of the

photons in the sample from the source to the scattering center and back to the detector respectively. The exponential factors are introduced to account for linear attenuation coefficients ( $\mu_1$  and  $\mu_2$ ) of the primary and scattered photons within the sample.

#### 4 Materials and Methods

The soil used in this study was collected in the experimental field of Pindorama, SP, Brazil, part of the Agronomic Institute of Campinas, inside a 5000m<sup>2</sup> area of combined Brazilian Podzol (Paleuhumult) and red-yellow Brazilian Latosol from Motuca-SP, Brazil. To calibrate soil bulk density measurements, a set of air-dried and sieved soil samples were placed in a number of 50x50x80mm Plexiglass boxes.

To calibrate soil water content measurements, a set of sieved soil samples with different moisture content was also put into a various 50x50x80mm Plexiglass boxes. This enabled us to study the quantity of photons backscattered with each energy E into a defined solid angle with some  $Z_{av}$ . The average atomic number  $Z_{av}$  was defined as:

$$Z_{av} = \sum_{i} w_{i} Z_{i}$$

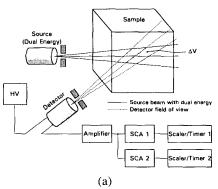
where  $w_i$  is the mass fraction of atom i and  $Z_i$  its atomic number, as found in the sample. Mixtures of varying percentages of each of the mentioned materials were then made.

The experimental set-up consisted of two radioactive sources, one of <sup>137</sup>Cs for soil bulk density measurements and the other of <sup>231</sup>Am for water content measurements, emitting gamma ray energies of 662keV and 60keV respectively. The counting geometry employed was designed to increase available incident flux and reduce experimental time required for a given counting precision. Activity of the radioactive sources during the experiment was 600mCi and 300mCi.

Figure 1 shows the dual-energy Compton scattering scanning system, which consists of two radioactive sources (one operating with 60keV and the second one with 662keV), and scintillator detector (NaI(Tl)) assembled over a mechanical ring device; two stepper motors, one for translation and one for vertical

shift of the sample; two electronic pulse counting and processing systems; a IBM-PC-Compatible microcomputer operating at 200MHz; collimators; and a video display for imaging.

Background counts for this experiment were estimated as the area within the Compton peak window in the absence of a scatterer. These were then subtracted from their respective scattered photon counts for the samples being measured. The counting time employed for each energy was 50 seconds per sampled point on the projection with a spatial resolution of 2mm, a total of 30 sampled points per projection and a total 10cm vertical displacement.



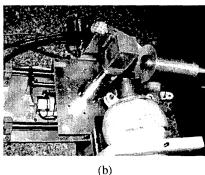


Figure 1 – (a) Dual-energy Compton Scattering System in Block Diagram; (b) Compton Scattering Scanning System with some details of the holder of the radioactives sources, detector, mechanical ring device, and collimators.

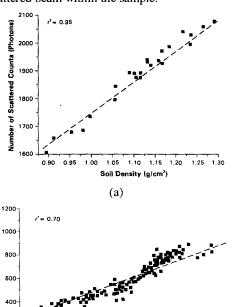
### 5 Results and Discussion

Figure 2 shows a plot of variation in number of scattered photons with soil density and water content at the

saturation thickness of a soil sample. This illustrates, as expected, a linear relationship between density, water content, and the number of photons Compton-scattered from a defined volume of the scatterer. However, two points must be made: although the data showed the expected linear relationships, they are obviously not on a straight line through the origin. There is an apparent positive intercept on the density axis, which varies with the average atomic number, estimated at 1.4 and 1.9g/cm<sup>3</sup> for the soil samples respectively. This is attributable to artifacts of measurement occasioned by the attenuation factors, and becoming more significant with increasing Z<sub>av</sub> and scattering angle; apart from the observed shift in the intercept on the density axis, a higher sensitivity was observed to changes in density at lower  $Z_{\rm av}$  values compared to higher ones. The Compton scattering coefficient decreases only weakly with the atomic number whereas the photoelectric coefficient is a power function of Z. The difference between these two coefficients is due to the fact that Compton scattering is a process defined for relatively weakly bonded electrons, the number of which is relatively constant with increasing atomic number. On the other hand, the photoelectric effect prevails for tightly bound electrons and hence strongly dependent on Z. Hence the most significant Compton effects are expected at low Z where a high Compton cross-section is combined with a low attenuation coefficient.

Figure 3 shows Compton images with 662keV of a representative Brazilian soil samples, packed into a plexiglass box. The image represent a longitudinal cross section of the sample, made possible by raster motion of data collection of the scanning system. In these image, we have displayed directly volex-by-volex variation of number of scattered photons by grey levels, where black represents the lowest density (air) and white the densest part of the soil sample. A closer study of the images shows some areas with low values for scattered photons to

the left of the image. This is due to unequal attenuation in the scattered beam modulated by the distance traversed by the scattered beam within the sample.



Pigure 2 – (a) Plot of variation of number of scattered photons with soil density at 662keV; (b) Plot of variation of number of scattered photons with soil moisture at 60 keV

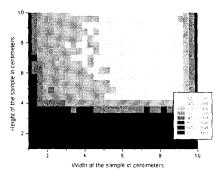


Figure 3 – A 662keV Compton image of soil sample with different bulk densities packed into a Plexiglass box, i.e., longitudinal cross sections.

For a better quantitative Compton scatter tomography, this problem requires additional correction factors. However, our preliminary results demonstrate that images obtained using this technique could have applications in soil science comparable to its transmission counterpart, opening the way to a possible a field measuring device based on Compton back-scatter photon detection technique.

#### 6 Conclusion

A dual energy Compton tomographic scanner dedicated to soil science studies has been designed and constructed at the Embrapa Agricultural Instrumentation Center, São Carlos, Brazil. This equipment, based on both <sup>137</sup>Cs and <sup>231</sup>Am radioactive sources, has been used to study dependence of scattered photons number on soil density and moisture. Linearity with linear regression coefficient of better than 0.95 has been obtained for soil density measurements. For water content measurements, linear regression coefficient was 0.70. The tomographic scan for a set of soil samples demonstrates the efficacy of this technique for soil density and moisture content measurements. Quantitative measurements were observed to be distorted by the effect of scattered beam attenuation. Results also shown the potentialities for continuing the development of this technique to be employed for in-situ soil study and should therefore be of particular interest to agriculture and industries.

## 7 Acknowledgement

The authors would like to express their appreciation to the Brazilian Enterprise for Agriculture Research (Embrapa), Brazilian Research Council (CNPq) and the Third World Academy of Science (TWAS) for a fellowship award and project SEP 12.098.800. We also thank Mr. V. Monzane and M. Sousa for help with drawing work.

#### 8 References

[1] Cormack A. M., "Reconstruction of Densities From Their Projections with Applications In Radiological Physics", *Phys.Med.Biol.*, v. 18(1973), N°. 2, p. 195-207.

- [2] Hounsfield G.N., "Computerized Transverse Axial Scanning (Tomography): Part 1. Description of System", *Brit.J.Radiol.* v.46(1973), p. 1016-1022.
- [3] Cho, Z.H. & Chan, J.K., "A Comparative Study of 3-D Image Reconstruction Algorithms with Reference to Number of Projections and Noise Filtering", *IEEE Trans. on Nucl. Science*, v. NS-21(1975), N°. 1, p. 344-364.
- [4] Webster, D. J., Lillicrap, S. C., "Coherent-Compton scattering for the assessment of bone mineral content using heavily filtered x-ray beams". *Phys. Med. Biol.*, v. 30(1985), p. 531-539.
- [5] Shakestaff, J., Morgan, H.M. and Lillicrap, S., "Gamma ray scattering for fat fraction measurement". *Phys Med. Biol.* 42(1997), 1403-1413.
- [6] Tatari, A., Casnati, E., Felsteiner, J., Baraldi, C. and Singh, B.," Feasibility of in-vivo tissue characterization by Compton scattering profile measurements". *Nucl. Instr. Methd.* B71(1992) p. 209-213.
- [7] Harding G., "Inelastic photon scattering: Effects and applications in biomedical science and industry". *Radiat. Phys. Chem.* v.50(1997), n. 1, p. 91 111.
- [8] Shukla, S. S., Karellas, A., Leichter, I., Craven, J.D. and Greenfield, M. A. "Quantitative assessment of bone mineral by photon scattering Accuracy and precision considerations". *Med. Phys.* v. 12(1985), p. 447-448.
- [9] Gigante, G. E., Hanson, A. L., "Evaluation of geometrical contribution to the spread of the Compton scatter energy distribution". *Phy. Rev A.*, 40(1989), no. 1, p. 171-180.
- [10] Stokes J. A, Alvar, K. R., Corey, R. L., Costello, D. G., John, J., Kocimski, S., Lurie, N. A., Thayer, D. D., Trippe, A. P., Young, J. C., "Some new applications of collimated photon scattering for non-destructive examination". *Nucl. Instr. Methd.* v. 193(1982), no. 1-2, p. 261-267.
- [11] Lawson, L. "Compton X-ray backscatter depth profilometry for aircraft corrosion inspection", *Mat. Eval.* v. 53(1995),no. 8, p. 936 941.
- [12] Holt, R. S., Cooper, M. J., and Jackson, D. F., "Gamma ray scattering techniques for non-destructive testing and imaging", *Nucl. Instr. Methd.* v. 22(1984), no. 1, p. 98-104.
- [13] Balogun, F. A, Spyrou, N. M., "Compton scattering tomography in the study of a dense material in a lighter

- matrix". Nucl Instr. Methds. B 83(1993), p. 533 538.
- [14] Arendtsz, N. V., Hussein, E. M. A., "Energy-Spectral Compton scatter imaging 2: Experiments". *IEEE Trans. on Nucl. Sci.* v. 42(1995), no. 6, p. 2166 2172.
- [15] Balogun, F. A, "Angular variation of scattering volume and its implications for Compton scattering tomography". *Appl. Radiat. Isto.* v. 50(1999), no. 2, p. 317 323.
- [16] Petrovic A.M., Siebert J.E., and Rieke P.E., "Soil Bulk Density Analysis in Three Dimensions by Computed Tomographic Scanning", *Aust. Journal Soil Res.*, v. 21(1982), p.445-450.
- [17] Hainswortth J.M. and Aylmore L.A.G., "The Use of Computer-Assisted Tomography to Determine Spatial Distribution of Soil Water Content", *Aust. Journal Soil Res.*, v. 21(1983) p.435-443.
- [18] Crestana S., Mascarenhas S., and Pozzi-Mucelli R.S.; "Static and Dynamic Three-Dimensional Studies of Wsater in Soil Using Computed Tomographic Scanning", *Soil Sci.*, v. 140(1985), N°. 5, p. 326-332.
- [19] Crestana S., Cesareo R., and Mascarenhas S., "Using a Computed Tomography Miniscanner in Soil Science", *Soil Sci.*, V. 142(1986), no. 1, p. 56-61.
- [20] Cruvinel P.E., "X and Gamma Ray Computerized Mini-Scanner for Multidisciplinary Use", Doctoral Thesis, (1987) University of Campinas, UNICAMP, SP, Brazil, pp. 329.
- [21] Cruvinel P.E., Cesareo R., Crestana S., and Mascarenhas S., "X and Gamma Rays Computerized Minitomograph Scanner for Soil Science", *IEEE Trans. on Instrum. and Meas.*, v. 39(1990), no. 5, p. 745-750.